lajss.org Latin American Journal of Solids and Structures
www.lajss.org

Stress-strain studies of cantilever sheet pile walls using 2D and 3D numerical simulations

Lucas Nogueira de Andrade[a*] https://orcid.org/0000-0002-9951-4938, Silvrano Adonias Dantas Neto[b] https://orcid.org/0000-0002-9951-4938

[a] Universidade Federal do Ceará, Campus Pici, Departamento de Engenharia Hidráulica e Ambiental, Fortaleza/CE, Brasil. E-mail: lucas.nogueira@alu.ufc.br
[b] Universidade Federal do Ceará, Campus Pici, Departamento de Engenharia Hidráulica e Ambiental, Fortaleza/CE, Brasil. E-mail: silvrano@ufc.br

* Corresponding author

Abstract
The purpose of this paper is to present the results of stress-strain analyses of cantilever sheet pile walls in which structural elements consist of spaced concrete piles considering the plane strain (2D) and triple stress (3D) states for the soil mass. The results show that there are significant differences in the stress and displacement distribution obtained in the 2D and 3D analyses of the retaining walls. It was observed that the 2D analyses did not allow for a satisfactory evaluation of the influence of the distance among the structural elements of the retaining wall on the evaluated stresses, while the 3D analyses indicated that there is an increase in the confining stresses as the distance among the piles decreased, responding to the formation of the arch-effect in cohesive soils. It was also observed that the horizontal displacements obtained in the 2D analyses were greater than those in the 3D simulations, suggesting a conservative tendency in the two-dimensional approaches for the analyzed structure. In general, it was observed that 3D analyses were more suitable for evaluating the stress-strain behavior of cantilever sheet pile walls consisting of spaced concrete piles, allowing a more realistic assessment of their performance in situations where the structural elements are spaced apart.

Keywords
Finite element method, cantilever sheet pile walls, arch-effect.

1 INTRODUCTION

As cantilever sheet pile walls are normally designed as elements based on theories considering the equilibrium of forces and moments of those resulting from the active and passive stress diagrams acting along the structure. However, in situations where the sites are formed by clayey soils it is common to use elements formed by adjacent spaced concrete piles. This occurs due to the arching tendency (Liang & Zeng, 2002; Chen et al., 2020), which consists of redistributing stresses from a yielding part of the soil mass to more rigid regions (Paik & Salgado, 2003; Liang & Yamin, 2009; Pardo & Sáez, 2014; George & Dasaka, 2021). This arching lends a local stability to the soil among the structural elements of the retaining wall, resulting in greater savings by reducing the number of required piles.

From the view of the stress-strain behavior, the retaining walls formed by continuous elements can be represented by a plane strain state status satisfactorily permitting the application of the limit equilibrium theories in their sizing. Such theories have a series of benefits, the most common perhaps being the simplicity of applying the existing analytical formulations such as methods widely used in Geotechnical Engineering. On the other hand, applying such methods do not permit obtaining a series of valuable data, which could mention the displacement field of the land and the actual sheet retaining wall.

When adopting the theories of limit equilibrium in designing the cantilever overlaid piles, the effect of spacing among the structural elements in the structure's behavior is normally considered by applying factors to reduce the passive stresses mobilized in the casting section (Alonso, 1983; Bowles, 1996), which depend on the sizes of the blueprint structural elements and the spacing adopted among them. Such a procedure might not realistically represent the stress-strain behavior of the retaining wall, since it should be considered that, with the formation of the arch-effect on the ground situated among the overlaid elements, there may be a redistribution of stresses and strains for which the which the plane strain condition ceases to be valid, directly affecting the structure's safety and deformation levels undergone this and the ground mass. In such situations, the 2D analyses (plane strain) would be unable to represent the arch-effect formation or stress-strain behavior in walls consisting of inter-spaced elements, which could only be assessed using stress-strain analyses that consider the triple status, as can be confirmed in several reports (Hong et al., 2003; Oliveira, 2014; Mollahasani, 2014).

From this viewpoint, the purpose of this article is to present the results obtained in 2D numerical simulations (plane strain state) and 3D (triple stress state) of the stress-strain behavior of a cantilever sheet pile wall formed by overlaid concrete piles in order to identify the conditions in which for the arch-effect formation occurs and its influence mainly on the distribution of stresses and on the soil mass displacements field. Moreover, a comparison was made among the state of stresses obtained from the numerical simulations undertaken (2D and 3D) with that obtained by analytical methods that consider the limit equilibrium condition of the soil mass.

2 MATERIALS AND METHODS

2.1 Description of the analyzed sheet wall structure

In order to assess the strain-strain behavior using 2D and 3D numerical simulations of a cantilever sheet pile wall consisting of overlaid concrete piles, an estimate was made of its length using theories of limit, considering that the aforementioned structure was designed to contain 4.50 m excavation, as illustrated in Figure 1, in which you can see the blueprint configuration of the piles indicating the spacing e and diameters (d) of the structural elements.

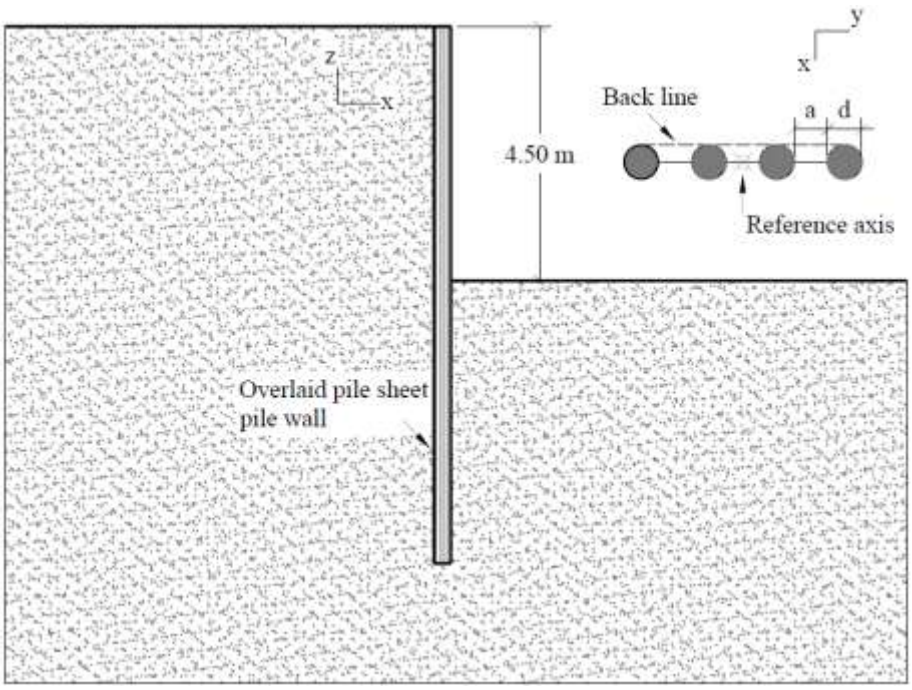

Figure 1 *Cross section for the analyzed cantilever sheet pile walls.*

To perform 2D and 3D numerical simulations, an isotropic homogeneous soil was considered, with a 30° effective internal friction angle, cohesion varying from 0 to 30 kPa, specific weight of 18 kN/m³, 0.3 Poisson coefficient, dilation angle of 0° and a Young Modulus of 20 MPa. The variation in values of the cohesion of the soil was calculated in order to assess their influence on the distribution of stresses and, consequently, on the formation of the arch-effect among the sheet pile wall's constituting structural elements.

In relation to the retaining wall, it was assumed that the structure is composed of circular concrete piles with a diameter of 30 cm. The dimensions of the piles fall within the range commonly used in containment projects, with a compressive strength of 20 MPa. The Young model and Poisson coefficient were estimated according to the NBR 6118/2023 criteria at 21 GPa and 0.2, respectively. The 2D and 3D numerical simulations were calculated considering spacing (a) among the constituent piles of the cantilever sheet pile walls varying from 0 to 40 cm.

2.2 Numerical Modeling

The RS2 and RS3 Rocscience software were used for the 2D and 3D numerical simulations, that apply finite elements method (MEF) to solve the governing equations.

2.2.1 Defining 2D numerical model

In situations in which the cantilever sheet pile walls are significantly higher than the excavation for which they were designed, it is expected that the displacement vectors have components only in the directions of the axes that define the structure's cross section, such as, for example, the x and z directions shown in Figure 1, which causes the soil behavior to be represented as a plane strain state. Thus, the 2D numerical models were developed considering the plane strain state that can be used satisfactorily to represent the behavior of the cantilever sheet pile walls analyzed in this paper when they consisted of continuous structural elements.

The finite element mesh used in the 2D simulations consists of 1436 six-node triangular elements. A mesh refinement study was conducted, and it was observed that increased refinement, compared to the mesh presented in this work, does not significantly impact the simulation results. Additionally, an automatic mesh optimization technique available in the RS2 and RS3 software was used to ensure simulation efficiency. In terms of boundary conditions, the displacement components were restricted in the x and y directions shown in Figure 2 on the horizontal plane representing the rigid layer, adopted at a depth of 20 m in relation to the ground surface and the horizontal displacement components on the sides of the numerical model, in order to represent a semi-infinite solid situation. It should be mentioned that no overloading was considered on the ground surface next to the excavation. Figure 2 shows the adopted boundary conditions, and the finite element mesh used in the 2D numerical simulations.

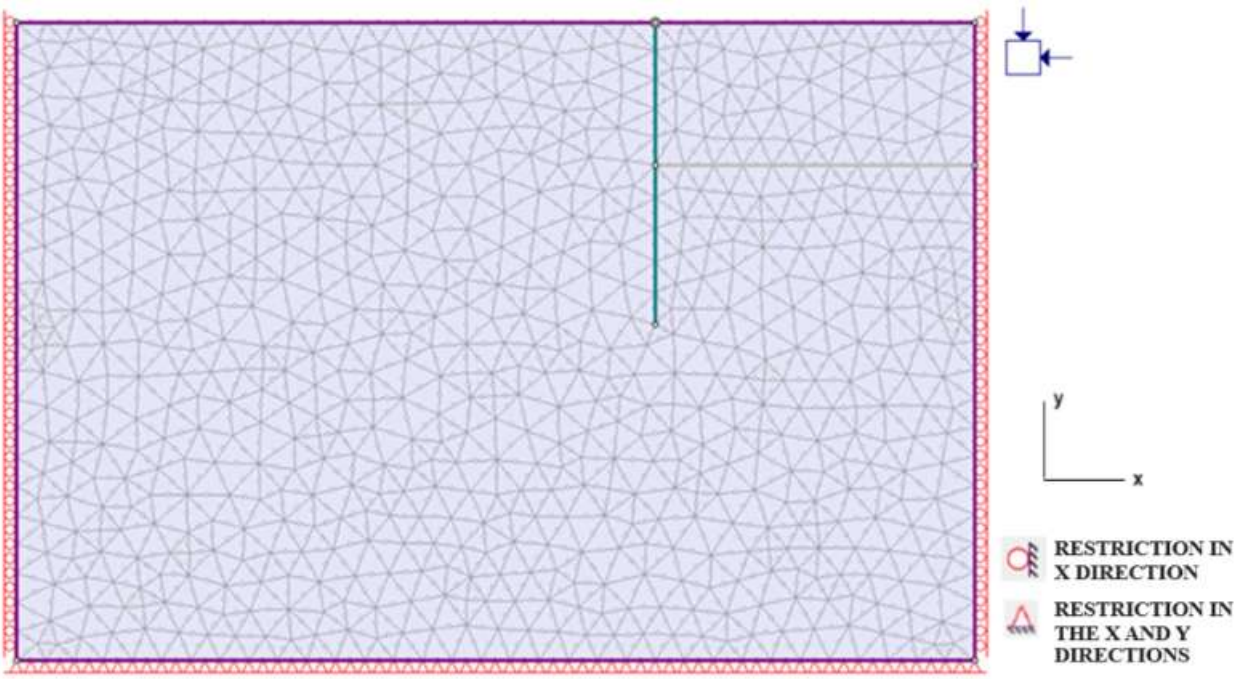

Figure 2 *Boundary conditions and mesh adopted for 2D model.*

The cantilever sheet pile wall in the 2D numerical model was represented considering a continuous structure consisting of beam elements and joint elements in the contact regions among the structure and the ground. To model the joint elements the Mohr-Coulomb sliding criterion was used with normal and shear rigidities of 100 MPa/m and 10 MPa/m, respectively. The continuous structure was modeled using a beam element defined by the Timoshenko criterion (1994), the properties of which are those mentioned previously for the concrete piles of the cantilever sheet pile wall.

To simulate the spacing among piles in the 2D analyses, it was necessary to implement an equivalent rigidity to represent each value adopted for the spacing among the structural elements of the cantilever sheet pile wall. This was done based on the consideration of equivalent values for the areas and moments of inertia representing the structural element in the 2D numerical simulations calculated by the Parallel Axis Theorem (Hibbeler, 2011) in line with the spacing adopted and geometry of the piles. This approach was adopted because in the 2D analyses performed on RS2, the structural elements are considered continuous, and therefore unable to represent a cantilever sheet pile wall consisting of separate interspaced circular piles. It is, therefore, essential to be considered in the plane strain analysis of a continuous structural element that has equivalent rigidity to that of the pile system for each considered spacing.

Table 1 shows the values adopted for the area (A) and moment of inertia (I) for each spacing adopted among the structural elements forming the cantilever sheet pile wall in the completed 2D numerical analyses.

Table 1 Areas and moments of inertia equivalent to 2D simulations.

a (m)	A (m^2/m)	I (m^4/m)
0.00	$2.36x10^{-1}$	$1.33x10^{-3}$
0.10	$1.77x10^{-1}$	$9.94x10^{-4}$
0.20	$1.41x10^{-1}$	$7.94x10^{-4}$
0.30	$1.18x10^{-1}$	$6.63x10^{-1}$
0.40	$1.01x10^{-1}$	$5.68x10^{-1}$

2.2.2 Defining 3D numerical model

In numerical model 3D, the boundary conditions were set more widely, as shown in Figure 3. On the horizontal plane representing the rigid layer (xy plane), the displacements were restricted in the directions of axes x, y and z. On the right front side (zy plane), restrictions were applied to displacement components in x and y directions, while on the left rear side (zy plane), restrictions were imposed on the displacement components in x and y directions. At the top, no displacement restraints were applied. On the two remaining sides parallel to zx plane, restrictions were applied only to the displacement component in the y direction.

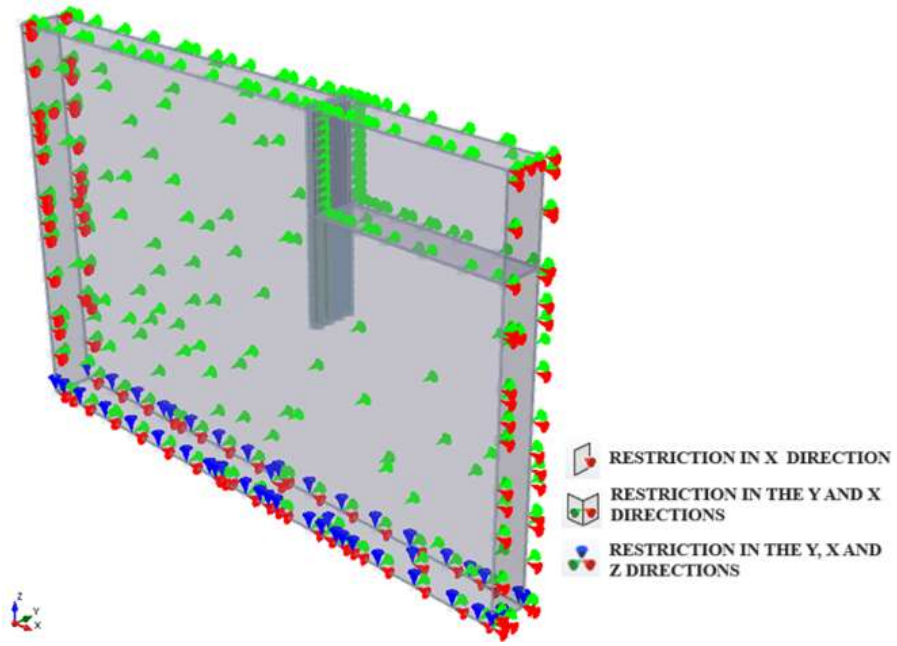

Figure 3 *Boundary conditions for model 3D.*

To create the finite element mesh for the 3D numerical model, four-node tetrahedron elements were used, undertaking a more refined discretization only in the regions closest to the piles that are of more interest to obtain the stress and strain field in the analyses performed as can be observed in Figure 4.

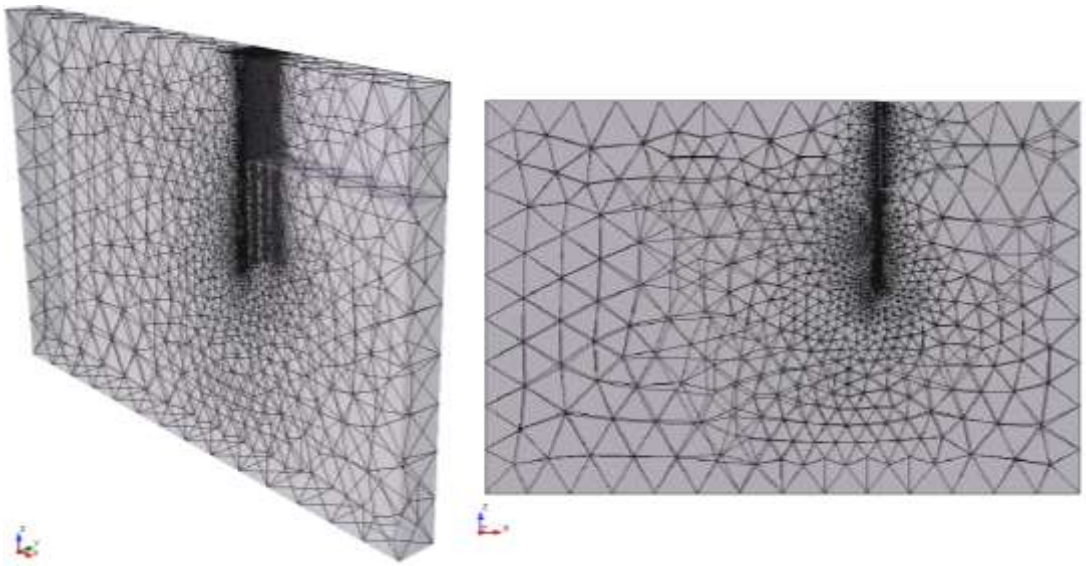

Figure 4 *Mesh adopted for 3D model.*

In the 3D numerical model, the adjacent circular elements (piles) of the sheet pile wall were based on combinations of individual Timoshenko beam elements (1994) with a thickness of 0.15 m distributed uniformly around the pile axis. Like the procedure undertaken when defining the 2D numerical model, joint elements were considered among the piles and the mass representing the ground with the aforementioned properties.

2.2.3 Constitutive model for soil

The Mohr-Coulomb perfectly plastic elastic model was adopted to represent the mechanical soil behavior in 2D and 3D numerical analyses, which provides satisfactory simplification for the stress x strain of the materials without hardening or softening during the plastic flow (Gurgel, 2012; Han et al., 2017). Moreover, it may be considered that this constitutive model is mostly adopted in Geotechnics Engineering (Liu et al., 2020) since it uses easy-to-understand and simple determinable geometric parameters, such as cohesion, friction angle, dilation angle, strain module and Poisson

coefficient (Gurgel, 2012; Oliveira, 2014). Also, its use implies results close to those measured on site and requires shorter computational time compared to other constitutive models (Medeiros, 2005).

3 RESULTS AND DISCUSSIONS

3.1 Dimensioning the cantilever sheet pile wall using limit equilibrium theories

Dimensioning filling the length of the wall on the ground used the Rankine theory (1857) to estimate the active and passive stress diagrams (Alonso, 1983; Bowles, 1996). This process consisted essentially of finding the necessary length to meet the static equilibrium conditions in terms of horizontal forces and moments of those resulting from the active and passive horizontal stress diagrams.

The most conservative shear strength parameters were considered to design the wall, namely, zero cohesion, friction angle equal to 30° and apparent specific weight of 18 kN/m³. Such conditions could be very easily applied to soft-to-medium compact sandy soils, such as those predominantly existing in Brazil's coastal regions. The calculations resulted in a total length of 9.50 m for the cantilever sheet pile wall.

3.2 Assessing the soil confined among the piles in the 3D numerical simulations

Figure 5 shows the distribution of the intermediate principal (σ'_2) and minor (σ'_3) effective stresses along the depth in the soil situated among the piles in the position indicated for the reference axis. The results were obtained considering 30 cm spacing among piles and for soils with cohesions equal to zero (C0) and 30 kPa (C30). The results indicate that for non-cohesive soil the spacing among constitutive piles of the retaining wall leads to a total deconfinement of the material represented by the nullity of the effective principal stresses σ'_2 and σ'_3 to -4.50 m in depth. For cohesive soil, it is noted that the effective principal stresses σ'_3 continue as zero along the depth, while there is an increase in the intermediate effective principal stresses σ'_2, indicating to be responsible for confining the soil among the pile elements, and consequently, by forming the arch effect.

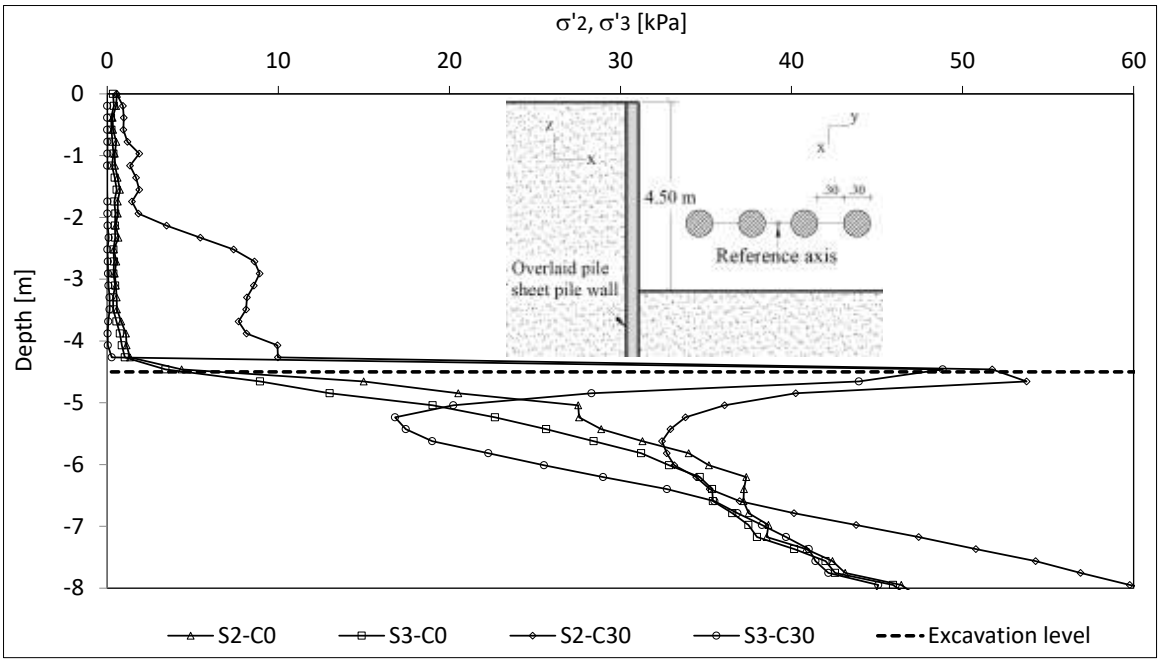

Figure 5 *Intermediate principal (σ'_2) and minor (σ'_3) effective stresses.*

Figure 6 shows the soil's plasticization levels along the depth on the excavation side. The results show that in the non-cohesive soil, for which the confining stresses σ'_2 are practically zero among the pile elements, the material is more plasticized. In such situations where the confining stresses are greater than zero, that is, those where the soil has a 30 kPa cohesion, the action of the confining stresses leads to a local stabilization of the soil among the piles due to the action of the confining stresses σ'_2, reflected in the lower level of plasticization noted. From those results, it can be said that the action of the intermediate principal stress σ'_2 produces an increase in the local stability in the materials among the structural elements of the retaining wall.

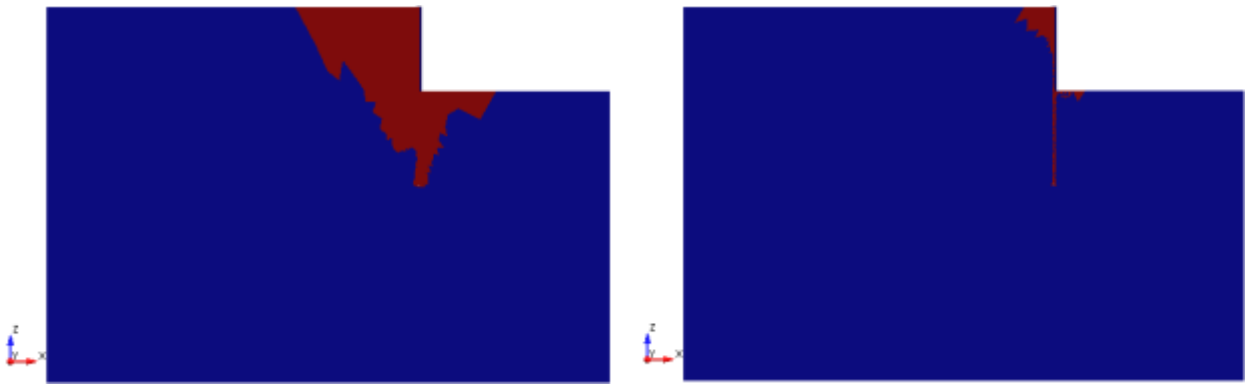

(a) (b)

Figure 6 *Plasticization of the soil among the pile elements: (a) Level of plasticization – c' = 0 kPa, (b) Level of plasticization – c'= 30 kPa.*

3.3 Assessing the arch-effect between adjacent structural elements

Table 2 shows the values of the effective principal stresses and the four-point stress tensor (P1, P2, P3 and P4) located as indicated in Figure 7 and situated at -1.00 m in depth in relation to the top of the retaining wall. These results were obtained considering the mass with effective cohesion of 30 kPa.

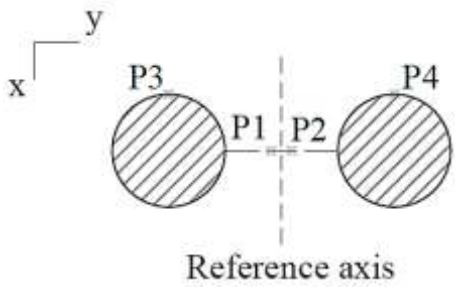

Figure 7 *Analysis points to define the principal directions in 3D simulations.*

Table 2 Stress components obtained in completed 3D simulations considering the joint elements – cohesive soil (C30).

POINT	σ'_1	σ'_2	σ'_3	σ'_{xx}	σ'_{yy}	σ'_{zz}	τ_{xy}	τ_{xz}	τ_{yz}
1	23.761	1.540	0.004	0.011	1.536	23.759	0.059	-0.080	0.130
2	23.955	1.684	0.007	0.013	1.686	23.946	-0.069	-0.131	-0.315
3	4.875	-0.019	-0.078	-0.075	-0.020	4.872	-0.011	0.068	-0.087
4	5.566	-0.024	-0.052	-0.059	-0.026	5.565	-0.003	0.054	0.018

Once known, the stress tensors at points P1, P2, P3 and P4 can be used to define the directions of the principal axes in line with the methodology presented in Chou & Pagano (1992). Table 3 presented the unit vector components that define the major principal ($\overrightarrow{n_1}$), intermediate ($\overrightarrow{n_2}$) and minor ($\overrightarrow{n_3}$) directions which are equal to the cosines of the direction angles indicated in brackets.

Table 3 Components and direction cosines of the unit vectors that define the main directions obtained in the analyses with joint elements – cohesive soil (C30).

POINT	$\overrightarrow{n_1}$			$\overrightarrow{n_2}$			$\overrightarrow{n_3}$		
	n_{1x}	n_{1y}	n_{1z}	n_{2x}	n_{2y}	n_{2z}	n_{3x}	n_{3y}	n_{3z}
1	0.003 (89.8°)	-0.005 (90.3°)	-0.999 (179.0°)	0.038 (88.0°)	0.999 (2.0°)	0.013 (89.0°)	0.997 (4.0°)	-0.043 (92.4°)	0.055 (86.8°)
2	0.005 (89.7°)	0.013 (89.2°)	-0.998 (178.8°)	0.042 (87.6°)	-0.999 (177.4°)	-0.016 (90.9°)	0.999 (2.5°)	0.045 (87.4°)	0.022 (88.7°)
3	0.013 (89.2°)	-0.017 (90.9°)	0.999 (2.5°)	0.179 (79.7°)	-0.983 (169.4°)	-0.011 (90.6°)	0.986 (9.6°)	0.16 (80.7°)	-0.017 (90.9°)
4	0.009 (89.4°)	0.003 (89.8°)	0.999 (0.8°)	0.182 (79.5°)	0.973 (13.3°)	0.139 (82°)	0.988 (8.8°)	0.146 (81.6°)	-0.046 (92.6°)

The results in Table 3 indicate that the major principal axis directions (1) at points P1 and P2 practically coincide with that of the Cartesian axis z, the intermediary (2) and minor (3) principal axes practically parallel to the horizontal plane xy, as illustrated in Figure 8a for point P1. Thus, it may be considered that in the central region among the structural elements of the wall there were few alterations to the principal directions in relation to due resting conditions, probably due to sliding among the materials favored by the presence of the joint element, causing increases in the insignificant shear stresses in the vertical planes yz and xy, as can be confirmed in the components of shear stresses acting on the ground in the position of points P1 and P2 in Table 3. It is also noted that the minor effective principal stresses (σ'_3) acting on the ground in positions of points P1 and P2 are practically zero, therefore confining the soil due only to the intermediate principal stress action σ'_2, the direction of which is practically the same as that presented by the longitudinal axis of the retaining wall.

Although in the region of the soil contained among the structural elements of the wall in the position of points P1 and P2, the soil having been confined by the action of σ'_2, the direction of which is practically the same as the axis y corresponding to the direction of the wall alignment, it is expected that there is greater obliquity towards the intermediary principal axis than to points closer to the retaining piles. This can be confirmed from the results in Table 3 for the directions of the intermediate principal axis in the positions represented by points P3 and P4, indicating a wider rotation in the intermediate principal direction around the vertical axis, as shown in Figure 8b. Therefore, it can be inferred that the intermediate principal axis tangents a curve whose geometry gives a sign of the region among the wall's structural elements where the material undergoes only the compressive stresses due to the σ'_2 action, and is, therefore, a sign of the arch-effect formation, as illustrated in Figure 8c.

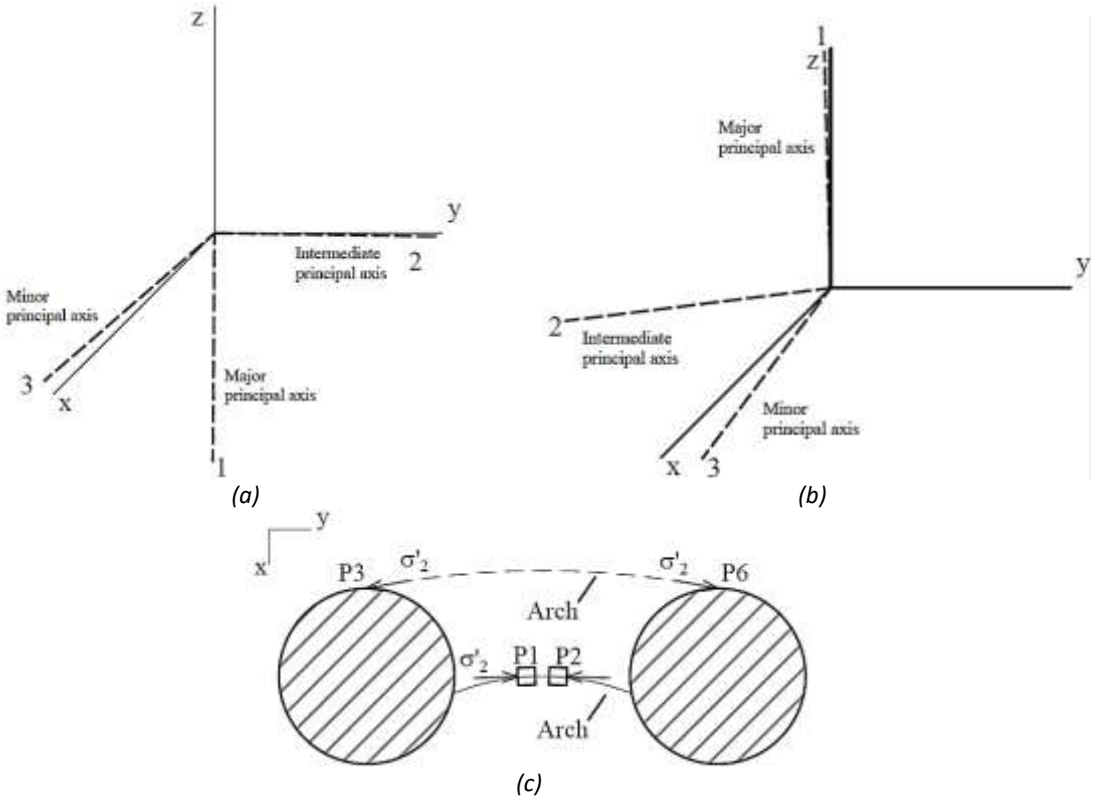

Figure 8 *Principal directions acting on the ground next to the retaining wall structural elements: (a) In P1 position, (b) In P3 position; (c) Formation of the arches among piles.*

It is worth mentioning that such results can only be obtained after undertaking stress x strain behavior simulations of cantilever sheet pile walls consisting of adjacent concrete elements using a model that helps define the triple stress state. Analyses that consider the plane strain state do not permit such an assessment due to the impossibility of obtaining the 3-D stress tensor and, consequently, the three stresses and principal directions.

3.4 Comparing results of the 2D and 3D numerical simulations 2D and 3D of the stress x strain behavior of the retaining wall

The stress x strain behavior of the wall was assessed considering the variation in depth of the values obtained from the confining stresses σ'_3 in the 2D analyses and σ'_2 in the 3D analyses, horizontal stresses from traditional analytical methods and for horizontal displacements.

For the horizontal displacements from the analytical formulations the Rankine methodology was used (1857) to calculate the active stresses acting on the excavation side to a depth of -4.50 m. For greater depths, that is, where the acting horizontal stresses are equivalent to those defined by the state of resting stresses, since there is little displacement mobilization. In this case, the horizontal stresses at rest were estimated by multiplying the effective vertical stresses by the thrust coefficient at rest estimated ion function of the internal friction angle of the ground according to Jacky's proposal (1944).

3.4.1 Influence of soil cohesion

Figure 9 shows the variation of the confining and horizontal confining stresses for the central position of the ground among the retaining wall piles in the position of the reference axis obtained in the 2D numerical simulations 2D (σ'_3), 3D (σ'_2) and from the deployed analytical formulations (theoretical) considering for the effective cohesion of the mass the following values: 0 (C0), 10 kPa (C10) - 30 kPa (C30).

It can first be noticeable that stresses σ'_3 obtained from the 2D simulations in the non-cohesive ground have a variation of approximately linear with depth, and therefore similar to those obtained for the estimated active stresses using the Rankine theoretical method (1957). However, the values obtained from the 2D numerical simulations were lower than those obtained by the analytical formulation used and indicates that the latter leads to major conservativism with regard to defining loads acting on the constitutive structural elements of the cantilever retaining wall.

On the other hand, comparing the results for the non-cohesive ground using the methodologies adopted, it is found that in the central region among the piles, the confining stresses σ'_2 there are practically zero 3D numerical simulations, the quite different from the results obtained in the 2D simulations and analytical formulations. This shows that the 2D analyses (numerical simulations and analytical formulations) of the cantilever wall as continuous elements do not satisfactorily represent the deconfinement that occurs in the cohesive soils when there is spacing among the constitutive structural elements of a cantilever sheet pile wall consisting of adjacent concrete piles.

Moreover, the results in Figure 9 show that there is an increase in intermediate effective principal stresses σ'_2 in the 3D simulations with cohesion along the excavation side, that is, to -4.50 m in depth, while, in 2D simulations, the behavior occurred inversely for the minor principal stress σ'_3. This is noticeable in the results in Figure 10 for a depth of -2.50 m in relation to the top of the retaining wall.

The increase in confining stresses with cohesion noted in the 3D simulations clearly indicates the tendency to form the arch-effect in the more clayey soils that is reflected in further local stability of the soil by the increase in σ'_2. However, it is noted that this tendency does not occur in an undefined manner, being observed in the analyses that, having increased, no longer occur in the confining stress values σ'_2. So, once again it is apparent that the stress x strain behavior obtained in 3D simulations for the cantilever interspaced adjacent piles is must better represented in the 3D simulations than in the models considering the plane strain in which the spacing among the structural elements of the wall is normally represented by a drop in the structure's rigidity, as mentioned herein above.

The results in Figure 9 show that the horizontal stresses acting on the wall to -4.50 m in depth estimated by Rankine's theory were higher than the stresses σ'_3 in the numerical models, indicating conservativism in the use of analytical formulations when designing the retaining walls. For greater depths, it is found that the stresses obtained in all numerical models were lower than the horizontal stresses obtained in the condition at rest, indicating that the use of such analytical methods could lead to unsatisfactory conditions of safety.

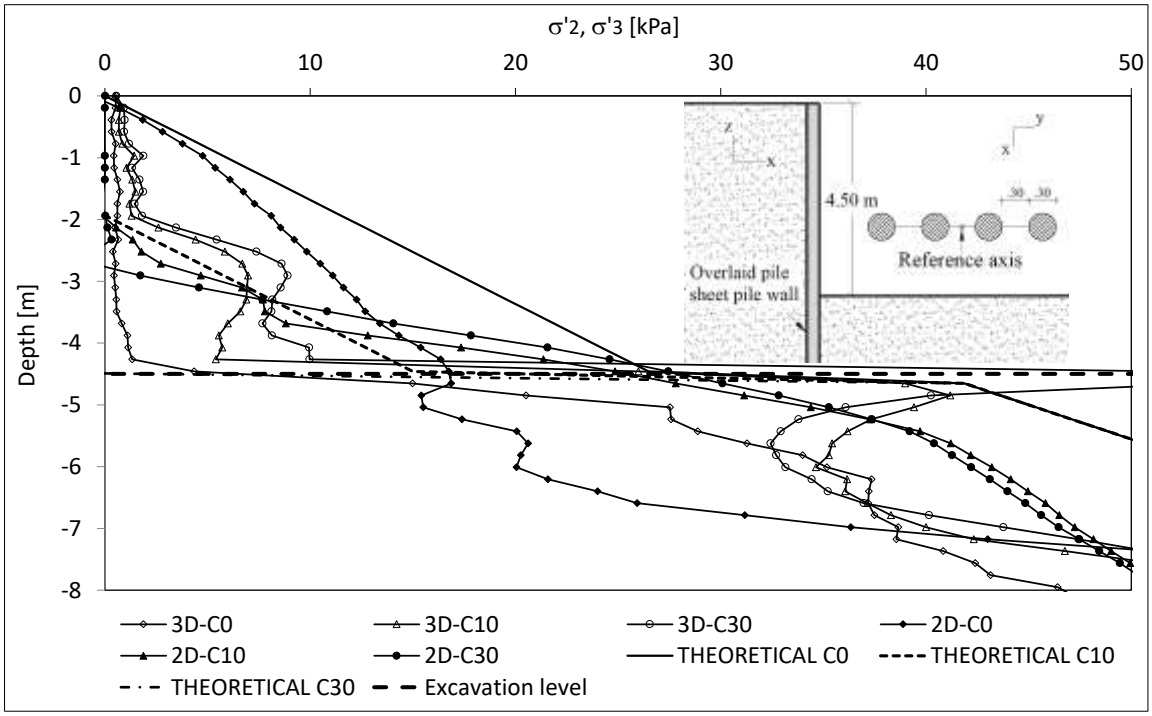

Figure 9 *Distribution of the intermediate (σ'_2), minor (σ'_3) effective principal stresses and horizontal stresses in the region of the existing soil among the piles for the different cohesion levels.*

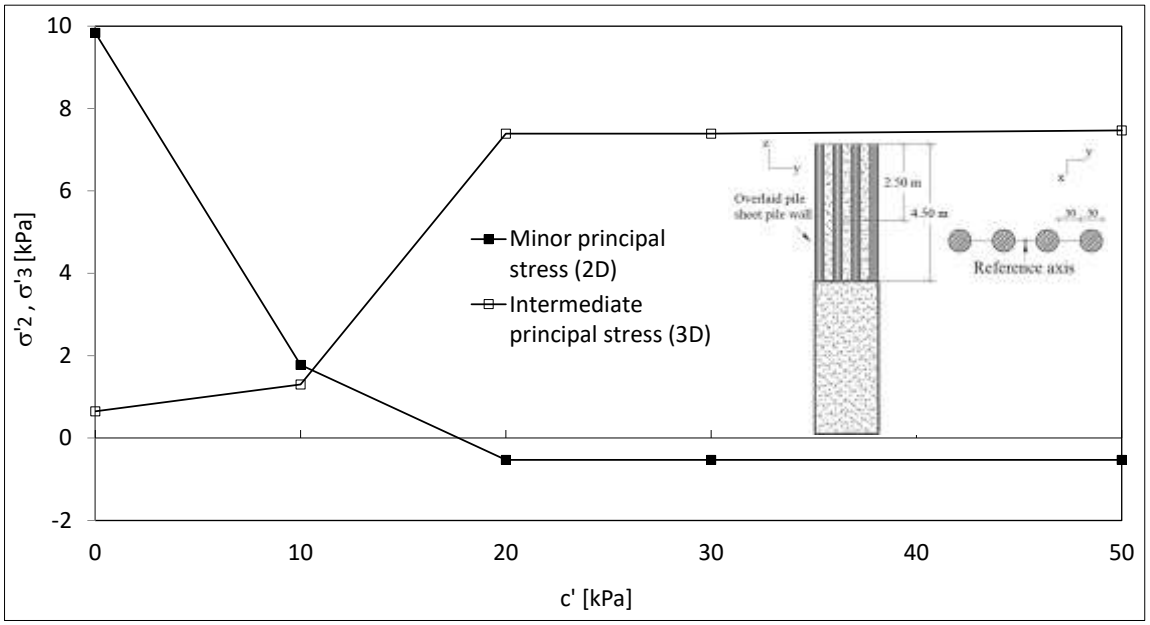

Figure 10 *Variation in confining stresses obtained in 2D (σ'_2) and 3D (σ'_3) simulations with cohesion are massif effective.*

3.4.2 Influence of spacing among piles

Figure 11 shows the distribution of stresses σ'_3, σ'_2 and horizontal stresses obtained in the 2D, 3D analyses and using analytical formulations, respectively. Such results were obtained for spacings equal to zero (E0), 10 cm (E10), 20 cm (E20), 30 cm (E30) and 40 cm (E40) among the constitutive structural elements of the cantilever retaining wall considering the non-cohesive soil.

It is relevant to emphasize that in the 3D numerical analyses where the soil has 0 kPa cohesion, it was not possible to reach the convergence of the numerical resulting process of the governing equations in cases where spacing among piles was 20, 30 and 40 cm, which was considered as a sign of generalized failures of the soil mass. This occurrence was also observed in the 2D analyses for 40 cm spacing.

The results shown in Figure 11 indicate that the 2D analyses were not sensitive enough to express the variation of the stress state with spacing among the structural elements represented by reducing the equivalent rigidity of the structure. On the other hand, in the 3D analyses, in general, it is apparent that there is a significant drop in the confinement level of the ground with pile spacing. These behaviors are more expressive when seeing the results of the confining stresses σ'_3 (2D analyses) and σ'_2 (3D analyses) in Figure 12 obtained for the average points among the piles of the retaining wall and a depth of -2.50 m.

Also, it is interesting to see in the results in Figure 11 that the curve related to the 10 cm spacing shows discontinuous points in the stresses. This behavior could be attributed to the arching effect, similarly to that found in the Terzaghi trapdoor test (1943), which occurs in the soil-structure interaction. As discussed by Oliveira (2014), the arching phenomenon is manifest due to the drop in rigidity in the regions among the piles. This decline in rigidity results in the localized reduction of the stresses, while at the same time causes an increase in the stresses in the regions situated in the rear (behind the piles), where the rigidity if more pronounced.

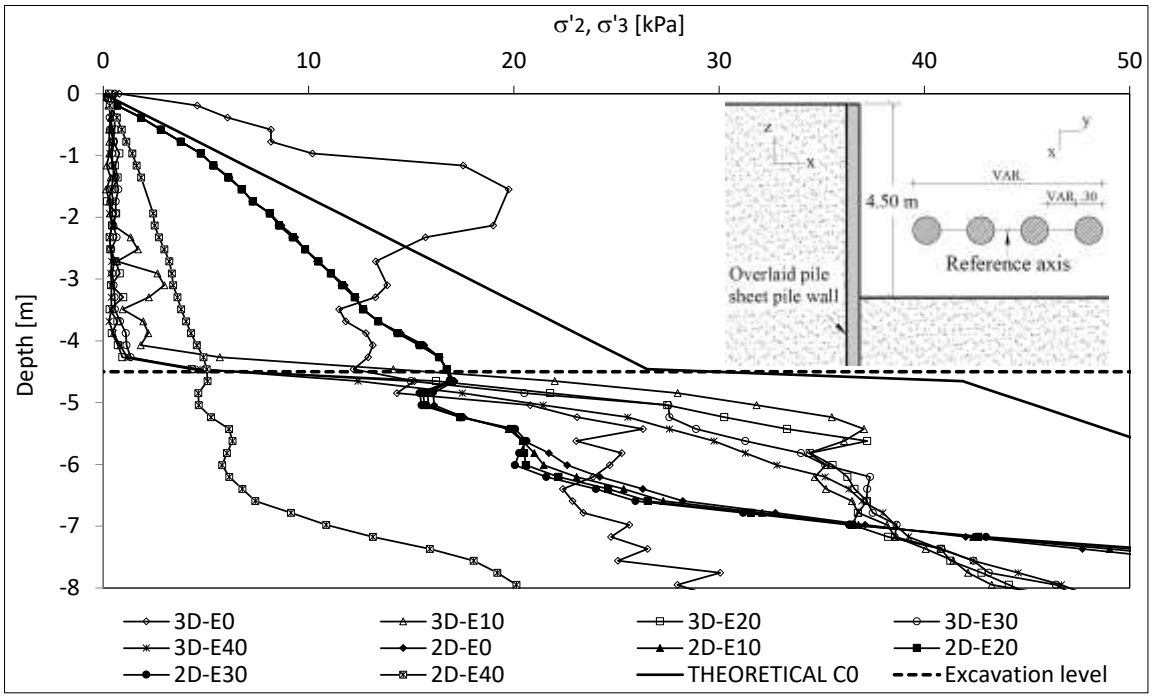

Figure 11 *Distribution of the intermediate (σ'_2), minor (σ'_3) effective principal stresses and horizontal stresses in the region of the soil existing among the piles for different spacing values among piles.*

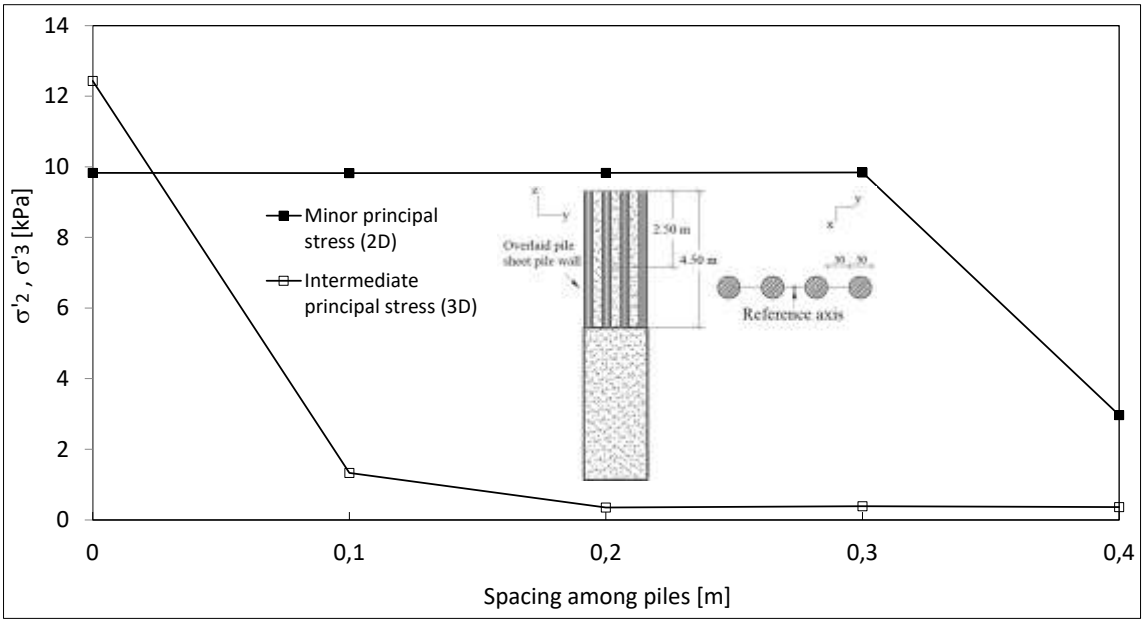

Figure 12 *Influence of spacing among piles in the intermediate (σ'_2) and minor (σ'_3) effective principal stresses obtained in 2D and 3D analyses, respectively.*

Figure 13 shows the variations of the horizontal displacements in direction x with the depth for different values for the spacing among constituent piles of the analyzed retaining wall, considering the non-cohesive soil mass. In accordance with these results, it is evident that the displacements are larger with the increase in spacing of the piles both in the 2D and 3D analyses. In general, it is found that the horizontal displacement in x direction in the 3D analyses was less compared to those in the bidimensional model in situations where the convergence of the numerical method was achieved, that is, for 0 and 10 cm spacings. This behavior was also seen in the analyses presented by Mollahasani (2014), Moreira (2016) and Ferreira (2019). However, this standard is no longer observed for 20, 30 and 40 cm spacings, where the convergence was not achieved, indicating major displacements and a possible generalized failure. Thus, it may be said that the numerical simulations without 2D are more conservative than those in 3D when the analyses reach an expected convergence resulting in the estimation of greater displacements. The reduction in horizontal displacement in x direction obtained in the 3D analyses can also be attributed to the arch-effect formation, since it is expected that in a situation where part of the soil mass undergoes higher levels of confinement, smaller displacements occur.

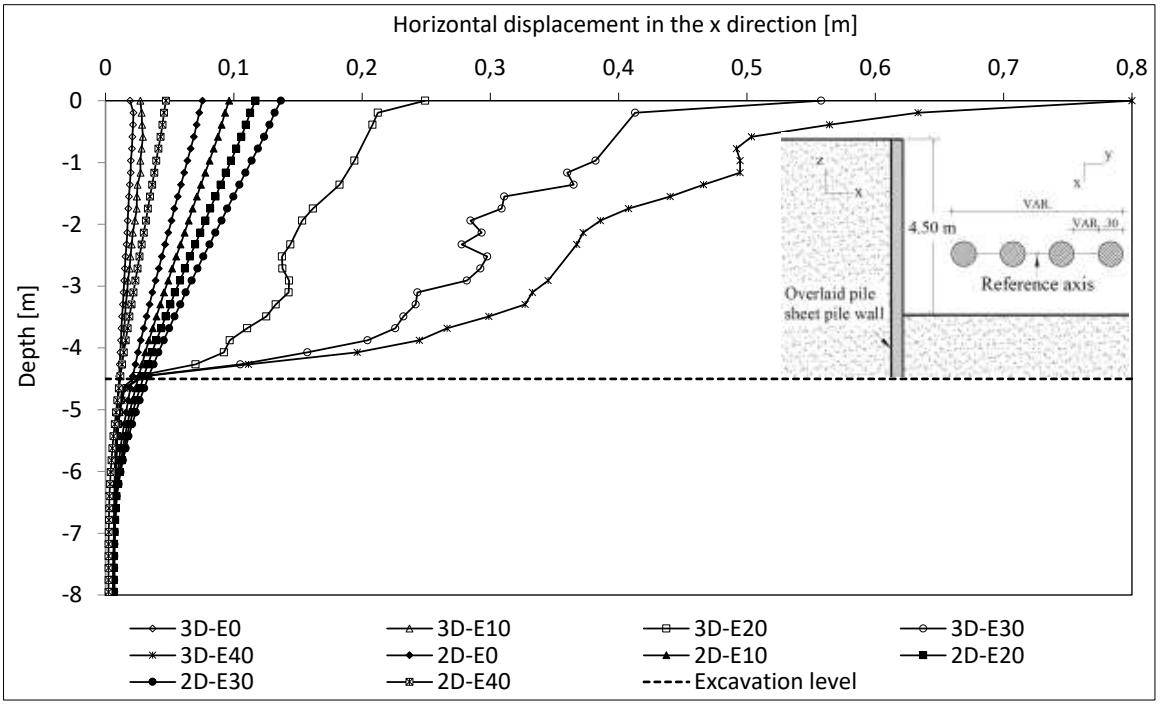

Figure 13 *Distribution of horizontal displacements in the region of the soil existing among the piles along the depth in line with the variation in spacing among piles considering the non-cohesive soil.*

4 CONCLUSIONS

In the analyses involving the simulations of the stress x strain behavior of the retaining wall for a deformation plane strain state (2D analyses) it was not observed in the significant variations in the stresses in relation to the changes in spacing among piles. This implies that, even with the change in the wall's rigidity, the bidimensional analysis cannot satisfactorily represent the discontinuity of the retaining structure in terms of redistributing stresses along the depth.

On the other hand, it is found that the numerical simulations of the stress x strain behavior considering the triple stress state (3D analyses) were able to satisfactorily represent the influence of the soil cohesion and spacing among piles in the values obtained for the intermediate principal stress (σ'_2) indicated as being principally responsible for the soil confinement and arc-effect formation among the retaining wall's structural elements. In general, the increase in the cohesive portion of the soil leads to an increase in the confining stresses in the soil existing among the pile elements. On the other hand, a high level of displacements enough based on a certain level for deconfinement that could characterize a generalized failure process in the soil existing among the retaining wall piles.

According to the results, it is evident that the confining stresses play a significant role on the displacements and level of plasticization of the soil mass among the retaining wall piles. This conclusion is clear when observing that, for cohesive soils, the effective principal stresses have lower values, resulting in displacement and a lower plasticization level. On the other hand, the non-cohesive soils, the effective principal stresses at the interface of the excavation are lower, resulting in greater displacements and a plasticization level in the soil mass.

Lastly, it can be concluded that in situations where the cantilever sheet pile walls consist of adjacent interspaced concrete piles, the results in numerical simulations that consider the plane strain state (2D analyses) do not satisfactorily represent the structure's behavior, nor in terms of stress development, the levels of displacements obtained, principally with regard to determining the influences of the spacing among piles at the levels of stresses and displacements in the ground. On the other hand, the numerical simulations of the stress x strain behavior of the cantilever wall consisting of adjacent concrete piles help provide information more consistent with the behavior of the retaining structure and permits a more appropriate assessment of key phenomena for their operation or stability, such as the formation of the arch-effect which is responsible for increasing local stability when the structures are implemented in clayey soils.

Author's Contribuitions:

Editor: Pablo Andrés Muñoz Rojas

Acknowledgments

Coordination for the Improvement of Higher Education Personnel (Capes) for financial support.

References

ABNT. Associação Brasileira de Normas Técnicas. NBR 6.118: Projeto de estruturas de concreto – procedimento. Rio de Janeiro, RJ: ABNT, 2023.

Alonso, U.R. (1983). Exercícios de Fundações. 13th reprint. São Paulo, SP, Brazil: Editora Edgard Blücher, 1983. 201p.

Bowles. J.E. (1996). Foundation analysis and design. United States. McGraw-Hill Companies. Inc.; 1996. 1207p.

Chen. G. Zou. L. Wang. Q. Zhang. G. Pile-Spacing Calculation of Anti-Slide Pile Based on Soil Arching Effect. Advances in Civil Engineering. v. 2020. 1-6. 2020. https://doi.org/10.1155/2020/7149379.

Chou, Pei Chi; Pagano, Nicholas J. Elasticity: tensor, dyadic and engineering approaches. New York: Dover Publications, 1992.

Ferreira, L.R. Análise numérica 3d de solo grampeado em solo sedimentar com inclusões verticais. 2019. 152 f. Dissertation (Master in Geotechnics), Geotechnics Post-graduation Program, University of Brasilia, Brasilia, DF, 2019.

George. T.I.; Dasaka. S.M. Numerical Investigation of Soil Arching in Dense Sand. International Journal Of Geomechanics. v. 21. n. 5. 1-16. 2021. http://dx.doi.org/10.1061/(asce)gm.1943-5622.0001971.

Gurgel, J.G.B. Modelagem numérica de estruturas de contenção atirantadas em areia. 2012. 169 f. Dissertation (master's in civil engineering). Federal University of Rio Grande do Norte. Natal-RN. 2012.

Han, J.Y; Zhao, W; Chen, Y. Jia, P.J.; Guan, Y.P. Design Analysis and Observed Performance of a Tieback Anchored Pile Wall in Sand.; Mathematical Problems in Engineering. V. 2017. p. 23. 2017. https://doi.org/10.1155/2017/8524078.

Hibbeler, R.C. Statics: Engineering Mechanics. São Paulo: Pearson Prentice Hall. 2011.

Hong, S.H; Lee, F.H; Yong, K.Y. Three-dimensional pile-soil interaction in soldier-piled excavations. Computers and Geotechnics. v. 30. n. 1. 81-107. 2003. http://dx.doi.org/10.1016/s0266-352x(02)00028-9.

Jacky, J. The coefficient of Earth pressure at rest. Journal of the Society of Hungarian Architects and Engineers. 355-358. 1944.

Liang, R.Y. Yamin, M. Three-dimensional finite element study of arching behavior in slope/drilled shafts system. Int. J. Number. Anal. Meth. Geomech.1157–1168. 2010. DOI: 10.1002/nag.851

Liang, R. Zeng, S. Numerical study of soil arching mechanism in drilled shafts for slope stabilization. Soils and Foundations. Japanese Geotechnical Society. v. 42. n. 2. 83–92. 2002.

Liu, M.; Wang, H.; Zhang, H. Analysis of pile spacing considering end-bearing soil arching and friction soil arching. In: ISCEG. 2020.

Medeiros, A.G.B. Análise Numérica de Estruturas de Contenção em Balanço e Grampeadas do Tipo "Estaca Justaposta" Assentes em Solo Poroso do DF. 2005. 157 f. Dissertation (Master in Geotechnics), Geotechnics Post-graduate Program, University of Brasilia, Brasilia, DF, 2005.

Mollahasani, A. Application of submerged grouted anchors in sheet pile quay walls. 2014. 125 f. Final Doctorate Exam (PhD in Civil and Environmental Engineering), University of Bologna, Bologna, Italy, 2014.

Moreira, P.S. Estudo de comportamento mecânico de uma cortina de estacas atirantada. 2016. 234 f. Dissertation (Master in Geotechnics & Transportation). Geotechnics & Transportation Post-Graduation Program, Federal University of Minas Gerais, Belo Horizonte-MG, 2016.

Oliveira, L.H.B. Modelagem numérica de uma estrutura de contenção de estacas espaçadas atirantadas em areia. 2014. 219 f. Dissertation (Master). Post-Graduation Program in Civil Engineering, Federal University of Rio Grande do Norte. Natal-RN, 2014.

Paik, K.H. & Salgado, R. Estimation of active earth pressure against rigid retaining walls considering arching effects. Geotechnique. v. 53. n. 7. 643–653. 2003.

Pardo, G.S. & Sáez, E. Experimental and numerical study of arching soil effect in coarse sand. Computers & Geotechnics, n. 57, 75-84, 2014.

Timoshenko, S. & Gere, J. Mechanics of Materials, Livros Técnicos e Científicos, 1994.

Terzaghi, K. Theoretical Soil Mechanics. New York: John Wiley & Sons. Inc..1943.